*Geosciences Journal*
Vol. 7, No. 3, p. 209 − 215, September 2003

# Framboidal pyrites in late Quaternary core sediments of the East Sea and their paleoenvironmental implications

Myong-Ho Park, Il-Soo Kim*, Byong-Jae Ryu

*Department of Earth System Sciences, Yonsei University, Shinchon-dong 134, Seodaemun-gu, Seoul 120-749, Korea*

*Korea Institute of Geoscience and Mineral Resources, Daejeon 305-350, Korea*

**ABSTRACT: The three piston cores, collected from the East Sea, were analyzed to detect changes of sedimentary environment during the late Quaternary. The cores consist mainly of muddy sediments that are interbedded with silty sands, lapilli and ash layers. The so-called dark laminated mud (DLM) layers are found during the last-glacial and interglacial transition. The geochemical results document that the DLM layers are enriched in Fe relative to Mn. Fe is present as a form of framboidal pyrite, which shows a proportion of about 2:1 for S and Fe. Based on the morphology, the pyrites are regarded to have grown in the transitional state between high and low supersaturations of Fe and S. Furthermore, the framboidal size distribution implies that the DLM layers have deposited in euxinic environments.**

**Key words:** framboidal pyrite, dark laminated mud, euxinic, late Quaternary, East Sea

## 1. INTRODUCTION

The East Sea is a semi-enclosed marginal sea between the Asian continent and the Japanese island arc, in which the late Quaternary sediments are characterized by decimetric to metric alternations of siliceous and calcareous muds (Chough et al., 2000; Bahk et al., 2000; Tada, 2002). The sediments of the western East Sea consists mainly of turbidite and hemipelagic muds, representing Marine-oxygen Isotope Stages (MIS) 1 to 3 (Bahk et al., 2000; Kim et al., 2003). At the upper part of hemipelagic facies, dark laminated mud (DLM) layers commonly occur. According to the previous study (Bahk et al., 2001), these DLM layers consist mainly of Mn-carbonates, with the average Mn/Ca ratio of 2.3, suggesting that the crystallites are mixed Mn-carbonates or Ca-rhodochrosites. Also, Bahk et al. (2000) suggested that the laterally continuous, non-porous laminated intervals of Mn-carbonate formed at the sediment-water interface rather than by a sub-surface diagenetic precipitation (see also Sternbeck and Sohlenius, 1997).

We found also the dark laminated mud layers in the cores of the East Sea, which can be correlative with the DLM layers, mentioned by Bahk et al. (2000, 2001). However, our preliminary results (KIGAM, 2002) indicate that the DLM layers are not composed of mixed Mn-carbonates. Therefore, (1) the main purpose of the present study is to identify the mineral composition and characteristic occurrence of the DLM layers. (2) Besides, we document general lithologic characteristics and establish a stratigraphic framework of the core sediments using tephrostratigraphic correlation with well-known eruption ages (Machida and Arai, 1983, 1992; Oba et al., 1995). (3) Finally, possible paleoenvironmental implications for formation of the DLM layers are discussed.

*Corresponding author: ilsookim@yonsei.ac.kr

## 2. MATERIALS AND METHODS

Three piston cores 01GHP-5, 01GHP-6 and 01GHP-7 were obtained from the northwestern part of the Ulleung Basin (Fig. 1). In the cores, tephra layers and other sedimentary facies were recognized by direct observations and partly confirmed by microscopic observations. For each tephra sample, glass shards of coarse fraction were examined under the scanning electron microscope (SEM). Major element compositions of volcanic glasses were analyzed on single glass shards using an energy-dispersive X–ray analyzer (EDX).

Core sediments from the laminated mud layers were also examined under the SEM to observe fine-grained minerals including framboidal pyrite. Fine structure and mineral composition of certain mud intervals such as pyrite-bearing DLM layers were observed with optical micrographs on polished thin sections of impregnated sediments. The impregnation was made through dehydration of wet sediments with acetone and embedding of the dehydrated sediments by Spurr low viscosity resin (Jim, 1985; Pike and Kemp, 1996). Element compositions of the DLM were determined on polished thin sections using a Microanalysis OXFORD (EDX) apparatus. Compositional variations across the DLM layers were analyzed by line measurement of relative concentrations of Fe, S, Mn, Al, and Si.

## 3. RESULTS AND DISCUSSION

### 3.1. Sedimentary Facies

The sediment cores consist predominantly of muddy sediments that are partly interbedded with silty sands, lapilli and ash layers (Fig. 2). The sediments are mostly olive gray

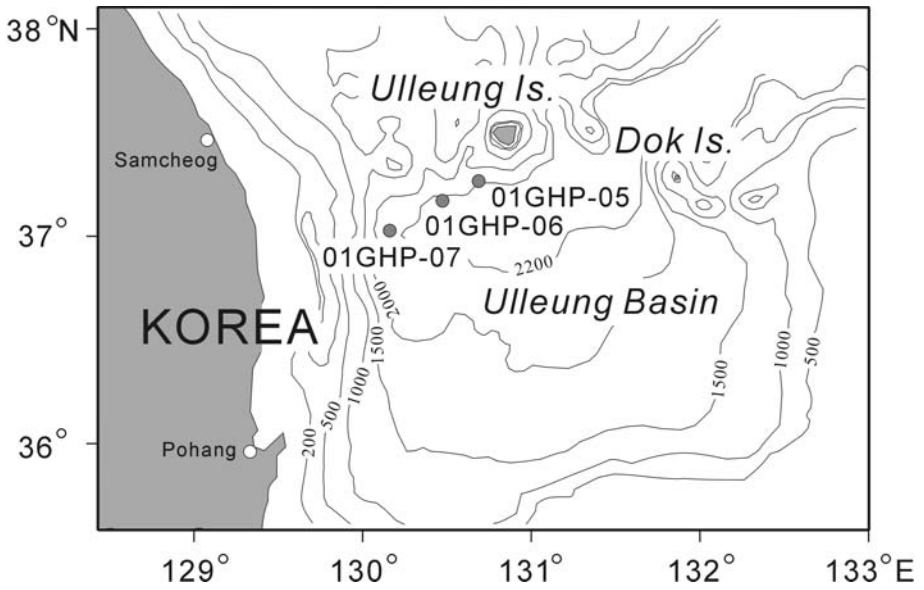


**Fig. 1.** Location of the three piston cores in the Ulleung Basin. Bathymetry in meters.

to dark olive gray (5GY 5/1 to 5GY 3/1), whereas the coarser sediments (silty sands or sandy muds) are more light-colored, light olive gray (5GY 7/1) to olive gray (5GY 4/1).

The cores consist of two types: hemipelagic and turbidite muds. The hemipelagic facies is dominated by bioturbated and crudely laminated mud, whereas the turbidite facies includes three mud types: (1) thinly laminated mud, (2) homogenous mud, and (3) alternating type with non-turbiditic facies. Thus, the muddy sediments in the cores are largely divided into four mud types: i.e., laminated mud, homogenous mud, crudely laimanated mud, and bioturbated mud (Fig. 2). In the laminated mud, laminae are mostly less then a few mm thick and consist of silt-clay couplets, while in the crudely laminated mud laminae are less sharp and not distinctly differentiated into silty and clayey ones. The most common mud type is the bioturbated mud, which is characterized by some burrow structures (circular, oval or tube shapes). Its thickness is very variable ranging from a few cm to more than 1 m. Some scattered foraminiferal shells and volcanic grains are often found. In 01GHP-7, the mud sequence is partly disturbed, probably during depositional processes such as slope failures of mass-flows (Fig. 2).

### 3.2. Tephra Layers and Stratigraphic Correlation

Several lapilli and ash layers were observed in three cores. The lapilli layers consist predominantly of white vesiculate pumices and massive-type glass shards associated with alkali-feldspar. Volcanic glass shards of these lapilli layers contain a high content of $Na_2O+K_2O$ (average 13.6 wt%) and a relatively small amount of FeO (average 0.9 wt%) (Table 1). And the massive-type glass shards of the lapilli layers belong to trachytic or phonolithic alkali composition (Fig. 3). In the cores, the upper and lower lapilli layers are correlative with the Ulleung-Oki (U-Oki) and Ulleung-Yamato (U-Ym) tephra layers as seen in Figugres 3 and 4 and Table 1 (see also Furuta et al., 1986; Machida and Arai, 1992; Park et al., 2003a, b).

In addition, some ash layers are found in the cores. These are characteristically high in $SiO_2$ content ranging from 78 to 79 wt%, but they are low in alkali contents. Among these, the rhyolitic ash layers (5.7 mbsf in 01GHP-6 and 3.9 mbsf in 01GHP-7) contain predominantly typical bubble-wall and/or plane-type glass shards (Machida and Arai, 1992; Machida, 1999; Gorbarenko and Southon, 2000; Park et al., 2003a). The morphology and geochemisty of volcanic glass shards, dispersed in the rhyolitic ash layers, suggest that these layers are correlative with the AT ash layer (Figs. 3 and 4; Table 1).

In the cores, DLM layers are useful for stratigraphic correlation. The previous $^{14}C$-age dating indicates that the DLM layer was formed during the last-glacial and interglacial transition (Fig. 2; Bahk et al., 2001). The average sedimentation rates between U–Oki and U–Ym (16.3 cm/kyr for 01GHP-5 to 27.6 cm/kyr for 01GHP-6) imply that the depth of DLM layer (ca. 14.5 ka) corresponds to about 2.9 mbsf in 01GHP-6 and about 2.4 mbsf in 01GHP-5, respectively. In fact, the characteristic mud facies of the dark laminated mud layers is found only between 2.5 and 2.6 mbsf in 01GHP-6 and between 2 and 2.1 mbsf in 01GHP-5. Thus, the dark laminated mud layers at these intervals are thought to be correlative with the DLM layers, mentioned by Bahk et al. (2000).

### 3.3. Framboidal Pyrites in the Dark Laminated Mud (DLM)

The facies of the DLM layers comprises 4–6 cm thick, dark olive gray (5Y 3/2) laminated mud with very dark brown bands (7.5YR 2.5/3). The planktonic foraminiferal

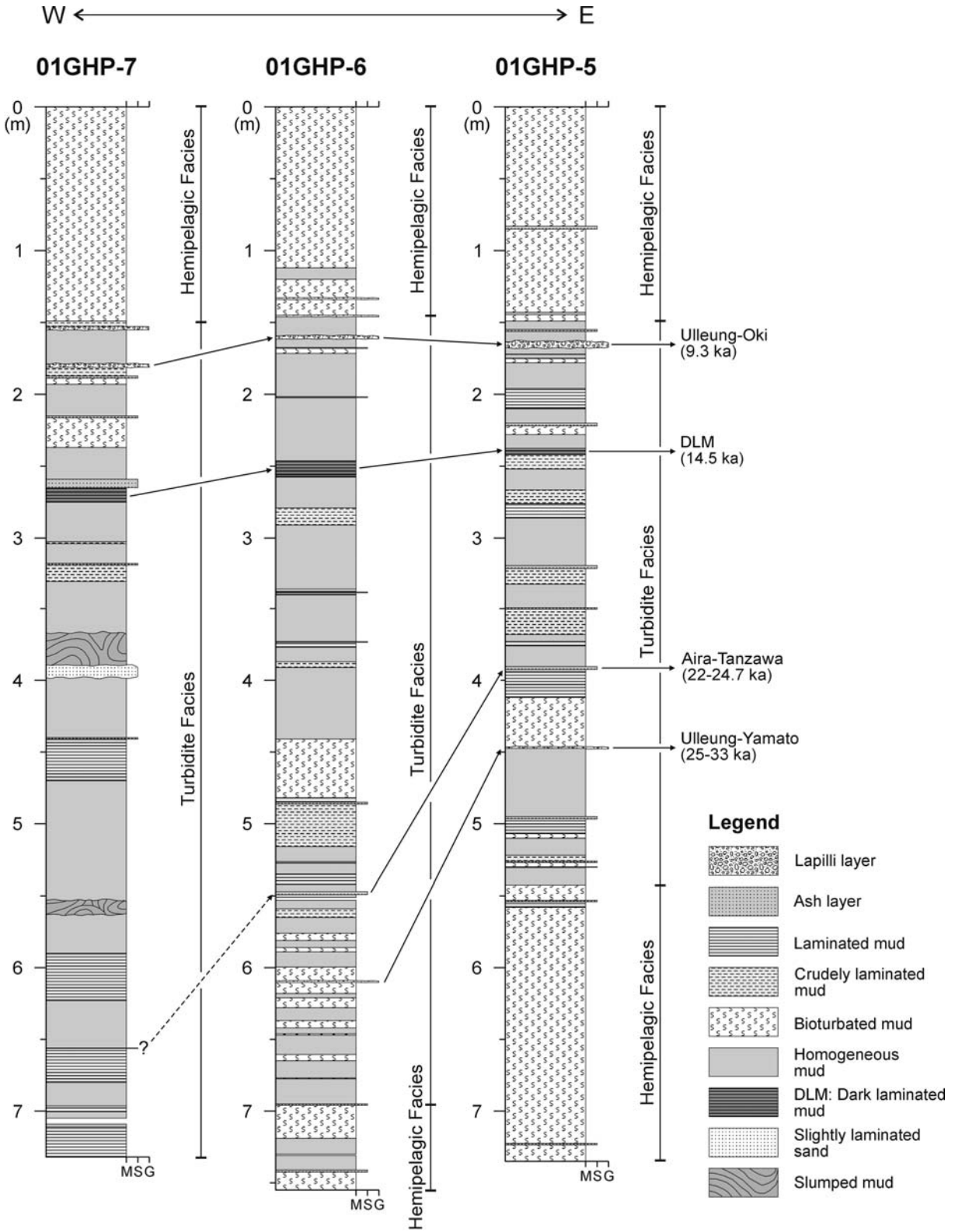


**Fig. 2.** Description of the piston cores and inferred stratigraphy correlation using tephra layers and $^{14}C$ absolute ages. $^{14}C$ ages of the DLM (dark laminated mud) layer taken from Bahk et al. (2001). M, S, and G indicate mud, sand, and gravel, respectively.

shells are often observed in the DLM intervals. The non-porous bands are 0.4 to 1.6 mm thick and laterally variable in thickness.

The line measurement of X–ray microanalysis shows that

**Table 1.** Average compositions of volcanic glass shards obtained in the study cores.

| Tephra layer | $SiO_2$ | $TiO_2$ | $Al_2O_3$ | FeO | MnO | MgO | CaO | $K_2O$ | $Na_2O$ | Reference |
|---|---|---|---|---|---|---|---|---|---|---|
| Ulleung-Oki | 64.39 | 0.13 | 19.56 | 1.02 | 0.07 | 0.26 | 0.75 | 7.20 | 6.62 | Park et al. (2003a) |
| | 63.78 | 0.37 | 19.16 | 2.21 | 0.11 | 0.21 | 1.16 | 5.92 | 7.08 | Park et al. (2003b) |
| | 64.67 | 0.12 | 19.45 | 0.93 | 0.06 | 0.25 | 0.71 | 7.11 | 6.70 | This study |
| | (2.11) | (0.18) | (0.50) | (1.08) | (0.08) | (0.55) | (0.36) | (2.07) | (2.06) | (n=28) |
| Aira-Tanzawa | 78.99 | 0.15 | 12.30 | 1.15 | 0.03 | 0.15 | 0.99 | 3.24 | 3.00 | Machida and Arai (1992) |
| | 78.23 | 0.11 | 12.42 | 1.20 | 0.06 | 0.15 | 1.00 | 3.36 | 3.48 | Park et al. (2003a) |
| | 75.80 | 0.14 | 13.61 | 1.03 | 0.10 | 0.13 | 0.68 | 4.48 | 4.03 | Park et al. (2003b) |
| | 78.37 | 0.13 | 12.35 | 1.21 | 0.07 | 0.13 | 0.98 | 3.39 | 3.37 | This study |
| | (0.98) | (0.10) | (0.41) | (0.18) | (0.06) | (0.09) | (0.14) | (0.25) | (0.80) | (n =15) |
| Ulleung-Yamato | 64.91 | 0.16 | 19.46 | 1.05 | 0.07 | 0.11 | 0.92 | 6.74 | 6.58 | Park et al. (2003a) |
| | 63.82 | 0.13 | 19.13 | 2.00 | 0.16 | 0.10 | 0.76 | 5.15 | 8.75 | Park et al. (2003b) |
| | 65.25 | 0.14 | 19.38 | 0.87 | 0.06 | 0.09 | 0.86 | 7.01 | 6.34 | This study |
| | (1.26) | (0.16) | (0.50) | (1.20) | (0.08) | (0.10) | (0.51) | (1.59) | (1.24) | (n =14) |

Analyses presented as a mean and standard deviation (in brackets). Normalized to 100% on a volatile-free basis. Total Fe expressed as FeO.

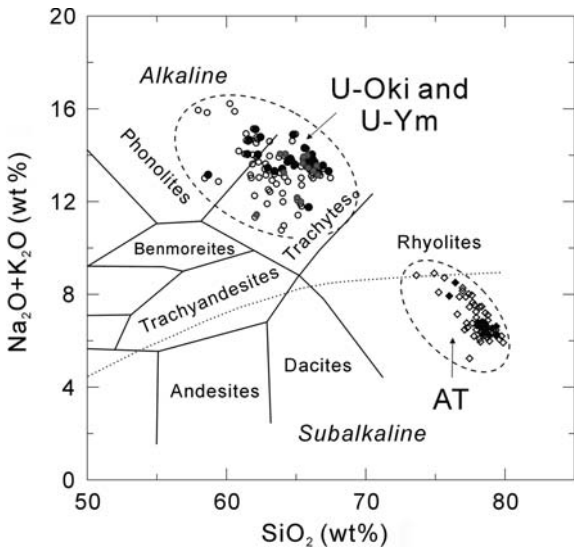


**Fig. 3.** Classification of the glassy tephra layers based on the total alkali-silica plot after Le Bas et al. (1986): *U−Oki* Ulleung−Oki (closed circles), *U−Ym* Ulleung−Yamato (gray circles), and *AT* Aira−Tanzawa (closed diamonds). The open shapes are from the previous data of Park et al. (2003a, b).

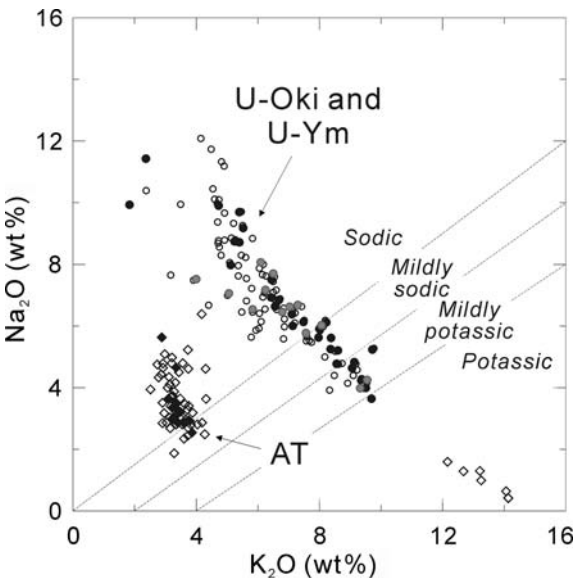


**Fig. 4.** Distribution of the Ulleung−Oki (U−Oki, closed circles), Ulleung−Yamato (U−Ym, gray circles), and Aira−Tanzawa (AT, closed diamonds) ashes in the diagram of $Na_2O$ *vs* $K_2O$. The diagram shows the more sodic and potassic characters of the Ulleung tephra layers than those of AT ash layers. The open shapes indicate the previous data of Park et al. (2003a, b).

Si and Al commonly occur in the DLM layers (Fig. 5). The previous element line-scan analysis (Bahk et al., 2001) shows that the DLM layers contain significant amounts of fine-grained silicates and/or aluminosilicates, and individual crystallites are mixed Mn-carbonates. However, at all depths of the DLM layers Mn is detected as a minor constituent, and the DLM layers are enriched in Fe relative to Mn. Therefore, these layers should be called as "pyrite-bearing laminated mud" rather than "Mn-carbonate mud."

In SEM views, the majority of pyrite is present as framboids, including both spherical and irregularly shaped aggregates of submicron-sized pyrite microcrystals (Fig. 6). The size of the framboidal aggregates varies between 4 and 12 mm in diameter (average 6.4 mm), whereas the size of individual crystals ranges from 0.4 to 1 mm. Framboid internal crystals are uniform, mainly as cubo-octahedron and often octahedron. The ratio of diameter of internal crystal to framboid is about 0.09. The SEM-EDX spectra document a proportion of about 2:1 for S and Fe in framboidal aggregates (Fig. 7).

### 3.4. Formation of Framboidal Pyrite in Euxinic Environment

In the DLM layers, pyrites are found as the cubo-octahedron and often octahedron crystals. The morphology of

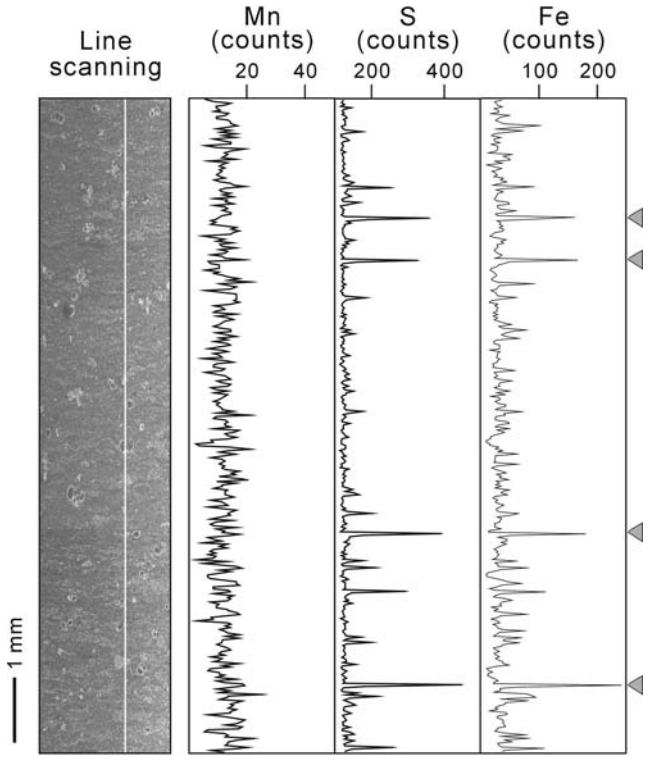


**Fig. 5.** Line measurements of the DLM layer. The element concentrations are given in relative intensity (counts/sec.). The measured line is marked on the microphotograph. The triangles on the right side indicate the core intervals enriched in pyrite.

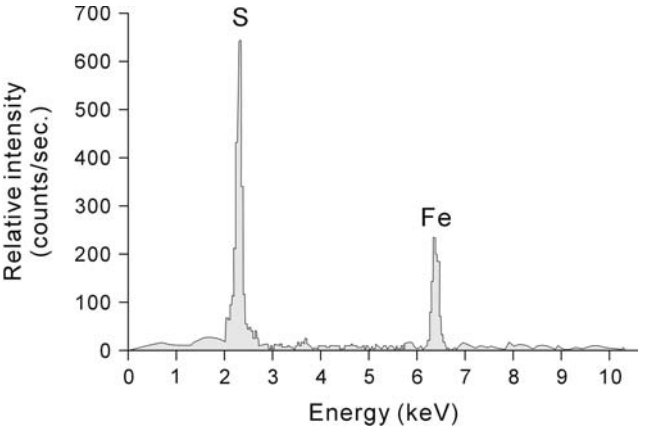


**Fig. 7.** SEM-EDX spectrum for a representative framboidal aggregate.

pyrite crystals is primarily dependent on solution saturation state during crystal growth (Wang and Morse, 1996). Cubo-octahedron to octahedron crystals imply that surface nucleation growth is assumed to be the dominant growth mechanism (Wang and Morse, 1996), suggesting that at the DLM intervals pyrites grow probably in the transitional state between high and low supersaturations of Fe and S.

On the other hand, according to Wilkin et al. (1996), the framboid size distribution may be used to indicate whether sediments were deposited under oxic or anoxic conditions. The plot of the mean and the standard deviation of framboidal size distributions suggests that the DLM layers of the three cores have formed under euxinic environments (Fig. 8). It is evidently different from the sediments of oxic (e.g., Wallops Island, GA) or dysoxic (e.g., Peru margin) environments but is probably rather less anoxic compared to the Black Sea (Fig. 8; Wilkin et al., 1996; Calvert et al., 1996; Wilkin and Arthur, 2001).

Accordingly, pyrite-bearing DLM layers in the cores evidently indicate the euxinic (anoxic and sulfidic) condition of the East Sea. However, the bottom-water conditions were changed from euxinic to more oxic during the transition between the latest Pleistocene and early Holocene (Oba et al., 1991, 1995). With such paleoenvironmental change in the East Sea, pyrite-bearing DLM layers occur no longer since Termination I.

## 4. CONCLUSIONS

1. The sediment cores consist predominantly of muddy sediments that are interbedded with silty sands, lapilli and ash layers. Among them, the muddy sediments are com-

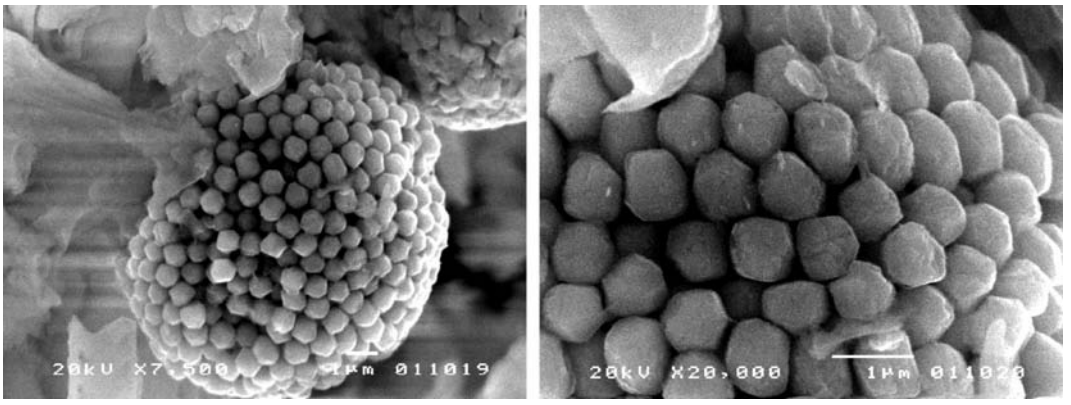


**Fig. 6.** Representative SEM microphotograph of framboidal pyrite observed in the DLM layers and its detailed view.

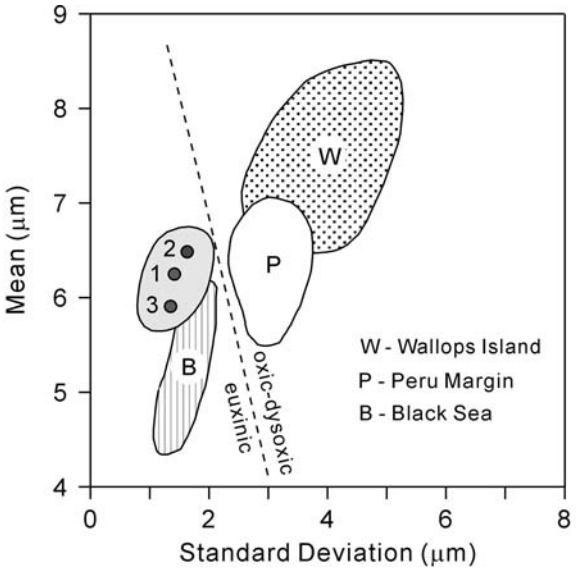


**Fig. 8.** The relationship between the mean and the standard deviation of average framboidal size. 1=01GHP-5, 2=01GHP-6, and 3=01GHP-7.

posed of two types of facies: The first type is hemipelagic facies, dominated by bioturbated mud and crudely laminated mud. The other type is turbidite facies, which includes thinly laminated mud and homogenous mud.

2. The lapilli layers consist mainly of white vesiculate pumices and massive-type glass shards associated with alkali-feldspar. According to EDX analysis, massive-type glass shards of the U-Oki tephra layers belong to trachytic or phonolithic composition. On the other hand, a rhyolitic ash layer consists mainly of bubble-wall and/or plane-type glass shards, which is correlative with the AT ash layer.

3. The geochemical results show that the interval of the DLM layers is enriched in Fe with a minor contribution of Mn.

4. In the DLM layers, Fe is predominantly present as a form of framboidal pyrite, which found as the cubo-octahedron and often octahedron crystals. Its morphology suggests that pyrite grows in the transitional state between high and low supersaturations. And the plotting of the mean and the standard deviation of the framboidal size distributions implies that the DLM layers have formed under euxinic environments.

**ACKNOWLEDGMENTS:** We thank Mr. Kim, J.H. of the Korea Institute of Geoscience and Mineral Resources. We thank also J.-B. Shin (Lab. Sedimentology, Yonsei Univ.) for his kind helps with SEM observation and X−ray microanalysis. The manuscript benefited from critical comments by Prof. Y.K. Sohn (Gyeongsang Natl. Univ.) and two anonymous reviewers. This study was supported by the Korea Research Foundation grant (KRF-2002-037-C00021).

## REFERENCES

Bahk, J.J., Chough, S.K. and Han, S.J., 2000, Origins and paleoceanographic significance of laminated muds from the Ulleung Basin, East Sea (Sea of Japan). Marine Geology, 162, 459−477.

Bahk, J.J., Chough, S.K., Jeong, K.S. and Han, S.J., 2001, Sedimentary records of paleoenvironmental changes during the last deglaciation in the Ulleung Interplain Gap, East Sea (Sea of Japan). Global and Planetary Change, 28, 241−253.

Calvert, S.E., Thode, H.G., Yeung, D. and Karlin, R.E., 1996, A stable isotope study of pyrite formation in the Late Pleistocene and Holocene sediments of the Black Sea. Geochimica et Cosmochimica Acta, 60, 1261−1270.

Chough, S.K., Lee, H.J. and Yoon, S.H., 2000, Marine Geology of Korean Seas. Elsevier, Amsterdam, 313 p.

Furuta, T., Fujioka, K. and Arai, F., 1986, Widespread submarine tephras around Japan: Petrographic and chemical properties. Marine Geology, 72, 125−142.

Gorbarenko, S.A. and Southon, J.R., 2000, Detailed Japan Sea paleoceanography during the last 25 kyr: Contraints from AMS dating and $\delta^{18}O$ of planktonic foraminifera. Palaeogeography Palaeoclimatology Palaeoecology, 156, 177−193.

Jim, C.Y., 1985, Impregnation of moist and dry unconsolidated clay samples using Spurr Resin for microstructural studies. Journal of Sedimentary Petrology, 55, 597−599.

KIGAM, 2002, Gas hydrate exploration and development in the East Sea. Annual Report KR-02-C-08, Korea Institute of Geoscience and Mineral Resources, Daejeon, p. 136.

Kim, I.-S., Park, M.-H., Lee, Y., Ryu, B.-J. and Yu, K.-M., 2003, Geological and geochemical studies on the Late Quaternary sedimentary environment of the southwestern Ulleung Basin, East Sea. Economic and Environmental Geology, 36, 9−15.

Machida, H., 1999. The stratigraphy, chronology and distribution of distal marker-tephras in and around Japan. Global and Planetary Change, 21, 71−94.

Machida, H. and Arai, F., 1983, Extensive ash falls in and around the Sea of Japan from large late Quaternary eruptions. Journal of Volcanology and Geothermal Research, 18, 151−164.

Machida, H. and Arai, F., 1992, Atlas of Tephra in and around Japan. University of Tokyo Press, Tokyo, 276 p.

Morse, J.W. and Emeis, K.C., 1990, Controls on C/S ratios in hemipelagic upwelling sediments. American Journal of Sciences, 290, 1117−1135.

Oba, T., Kato, M., Kitazato, H., Koizumi, I., Omura, A., Sakai, T. and Takayama, T., 1991, Paleoenvironmental changes in the Japan Sea during the last 85,000 years. Paleoceanography, 6, 499−518.

Oba, T., Murayama, M., Matsumoto, E. and Nakamura, T., 1995, AMS-$^{14}C$ ages of Japan Sea Cores the Oki Ridge. The Quaternary Research, 34, 289−296.

Park, M.-H., Kim, I.-S. and Ryu, B.-J., 2003a, Stratigraphy of late Quaternary core sediments and comparative study of the tephra layers from the northwestern Ulleung Basin of the East Sea. Economic and Environmental Geology, 36, 225−232.

Park, M.-H., Kim, I.-S. and Ryu, B.-J., 2003b, Distribution of late Quaternary tephra layers in the western part of the Ulleung Basin, East Sea. Geosciences Journal, 7, 123−127.

Pike, J. and Kemp, A.E.S., 1996, Preparation and analysis techniques for studies of laminated sediments. In: Kemp, A.E.S. (ed.), Palaeoclimatology and Palaeoceanography from Laminated Sediments. Geoloical Society Special Publication, 116, 37−48.

Sternbeck, J. and Sohlenius, G., 1997, Authigenic sulfide and carbonate mineral formation in Holocene sediments of the Baltic Sea. Chemical Geology, 135, 55−73.

Tada, R., 2002, Asian monsoon evolution and its impact on the Japan Sea paleoceanography. Korea−Japan Symposium, Gyeongju,

September 26–28, p. 101–106.
Wang, Q. and Morse, J.W., 1996, Pyrite formation under conditions approximating those in anoxic sediments: I. Pathway and morphology. Marine Chemistry, 52, 99–121.
Wilkin, R.T. and Arthur, M.A., 2001, Variations in pyrite texture, sulfur isotope composition, and iron systematics in the Black Sea: Evidence for Late Pleistocene to Holocene excursions of the $O_2$–$H_2O$ redox transition. Geochimica et Cosmochimica Acta, 65, 1399–1416.
Wilkin, R.T., Barnes, H.L. and Brantley, S.L., 1996, The size distribution of framboidal pyrite in modern sediments: An indicator of redox conditions. Geochimica et Cosmochimica Acta, 60, 3897–3912.

Manuscript received June 13, 2003
Manuscript accepted August 30, 2003